Regular Article

PHYSICAL CHEMISTRY RESEARCH
Published by the
Iranian Chemical Society
www.physchemres.org
info@physchemres.org

Phys. Chem. Res., Vol. 12, No. 4, 1079-1090, December 2024
DOI: 10.22036/pcr.2024.458030.2528

The Interaction of Sulfamethoxazole Drug with the Pristine and Functionalized C_{60} Fullerenes: A DFT Study

M. Soleymani[a], H. Dashti Khavidaki[b,*] and H. Yarahmadi[b]

[a]*Biosensor and Energy Research Center, Faculty of Basic Science, Ayatollah Boroujerdi University, Boroujerd, Iran*

[b]*Department of Chemistry, Faculty of Basic Science, Ayatollah Boroujerdi University, Boroujerd, Iran*

(Received 17 May 2024, Accepted 11 September 2024)

Adsorption properties of sulfamethoxazole drug on the pristine (C_{60}) and functionalized ($C_{60}HNH_2$) fullerenes in different situations were calculated by density functional theory calculations using the ωB97XD method and 6-31G(d) standard basis set in gas and solution phase. Based on the adsorption and Gibbs free energies, the adsorption of sulfamethoxazole on the pristine C_{60}, in all situations, was unfavorable, but its adsorption on the functionalized fullerene was spontaneous and favorable, in two situations. Also, in agreement with the Gibbs free energy data, functionalized fullerene has negative solvation energy in two situations, therefore, it can be suitable as a nano-carrier in drug delivery systems. In addition, the nature of interaction between sulfamethoxazole and functionalized fullerene in the most favorable situation was analyzed by the independent gradient model based on Hirshfeld partition (IGMH). The [4+2] cycloaddition reactions of **SMX** with the fullerenes were also studied and the results ruled out the possibility of chemical adsorption *via* such reactions.

Keywords: Sulfamethoxazole, C_{60} fullerene, Functionalization, DFT, Adsorption, Drug delivery

INTRODUCTION

Drug delivery is a nanotechnology method in medicine to improve the drug solubility and its lifetime, to control the drug release in the vivo tissues, and eventually to design safe and effective drugs [1-6]. It has been found that the fullerenes are appropriate candidates for drug delivery systems due to their properties such as unique spherical structure, hydrophobic characteristic, less side effects in the body tissue, and efficient drug loading. Among fullerenes, C_{60} is the most stable and the most abundant and has received more attention in drug delivery [7-14].

So far, the interaction of different drugs on fullerene C_{60} and its derivatives has been investigated, including amantadine [5], arginine, leucine, and tryptophan [15], cyclophosphamide derivatives [16], 5-fluorouracil [17], amphetamine [18], adenine [19], favipiravir [20], phenylpropanolamine [21], temozolomide, procarbazine, carmustine, and lomustine [22], hydroquinone [23], penicillamine [24], metronidazole [25], ornidazole [26], and cyclopropylpipezarine [27].

In addition, Salimi *et al.* [28] studied the adsorption properties of letrozole drug onto pristine and Ge- and Si-doped C_{60} fullerene in different states in both gas and solution phases by using DFT calculations (B3PW91 method and 6-311G(d,p) basis set. They concluded that letrozole incorporating Si-doped C_{60} can be considered as a drug delivery system. The interaction of gemcitabine drug with C_{60} and C_{70} fullerenes was also investigated by Ashrafi and his coworkers [29] using DFT calculations at a B3LYP/ccpvdz level, and the ability of these Al-doped fullerenes to deliver gemcitabine was demonstrated. Besides, Bagheri Novir *et al.* [30] studied the interaction of chloroquine, as an effective drug in the control of COVID-19 infection, with pristine and B-, Al-, Si-doped C_{60} fullerenes. Based on their studies, Al-, Si-doped fullerenes can be

*Corresponding author. E-mail: dashti@abru.ac.ir

considered as the better drug delivery for chloroquine. Meanwhile, the interaction of metformin drug with C_{60}, C_{48}, and doped fullerenes was performed by Ebrahimzadeh Rajaei and his coworkers [31] using density functional theory at the level of B3PW91 and 6-311G(d,p) basis set in both gas and solvent phases. They concluded that among the studied fullerenes, SiC_{59} can be extended as a drug delivery system for metformin.

Sulfamethoxazole (**SMX**) (Scheme 1) is a sulfa drug and a common antibiotic which have been widely used for the treatment of bacterial infections in humans, such as prostatitis, bronchitis, and urinary tract infections. **SMX** inhibits the formation of the dihydropteroate synthase enzyme, thus, preventing the synthesis of folic acid and therefore, stops the bacterial growth [32,33].

The aim of this work is to investigate the interaction between sulfamethoxazole drug and the pristine and HNH_2-functionalized C_{60} fullerenes in both gas and solvent (water) phases by DFT using ωB97XD method and 6-31G(d) standard basis set. Also, the structural and electrical properties variations are calculated for different adsorption situations of **SMX** on the C_{60} and $C_{60}HNH_2$ fullerenes before and after the adsorption, to find the best drug situation for the drug delivery system. In addition, the possibility of using pristine and functionalized C_{60} fullerene as the drug delivery system is evaluated.

Methods

All calculations were performed by using the Gaussian 09 program [34]. The structure of sulfamethoxazole drug, C_{60}, $C_{60}HNH_2$, transition states, and cycloadducts was optimized using ωB97XD method and 6-31G(d) standard basis set. While the absence of any imaginary frequencies confirmed the geometrical minima of sulfamethoxazole drug, C_{60}, $C_{60}HNH_2$, and cycloadducts, the transition states showed one imaginary frequency.

The adsorption energy (E_{ads}) of the sulfamethoxazole drug and the pristine and functionalized fullerenes was calculated using the Eq. (1):

$$\Delta E_{ads} = E_{complex} - (E_{\mathbf{SMX}} + E_{fullerene}) \quad (1)$$

where E_{SMX}, $E_{fullerene}$, and $E_{complex}$ refer to the energies of the sulfamethoxazole, the pristine or functionalized fullerene, and **SMX**+fullerene complex, respectively.

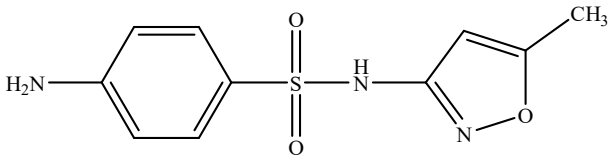

Scheme 1. Chemical structure of sulfamethoxazole

Furthermore, the polarizable continuum model (PCM) was used to study the effect of the solvation effect of water on the interactions of fullerenes. This reliable model is widely used to investigate the solvent (such as water) effects on molecular properties [35-40]. The stability of complexes was determined by calculating the solvation energy (ΔE_{solv}) using the Eq. (2) [41]:

$$\Delta E_{solv} = E_{solution} - E_{gas} \quad (2)$$

where $E_{solution}$ is the total energy of the compound in the solution phase and E_{gas} is the total energy of the compound in the gas phase.

In addition, the independent gradient model based on Hirshfeld partition (IGMH) analysis was carried out by using Multiwfn software [42].

Natural population analysis (NPA) was applied to calculate the natural atomic charges and the global electron density transfer (GEDT) values [43,44].

RESULTS AND DISCUSSION

To Find the Most Stable Conformer of SMX

It seems that **SMX** has two important conformers including eclipsed and staggered, in which the two aromatic are mutual and away from, respectively. Thus, at the first step, a conformational analysis was performed on the molecule over the Cph-S-N-Cox dihedral angle (ox refers to the oxazole ring), in which the molecule was rotated by 5° in each step around this dihedral angle for a complete 360° cycle and the molecular energy was calculated. Figure 1 displays the diagram of the molecular energies of **SMX** relative to the C_{Ph}-S-N-C_{ox} dihedral angle rotation.

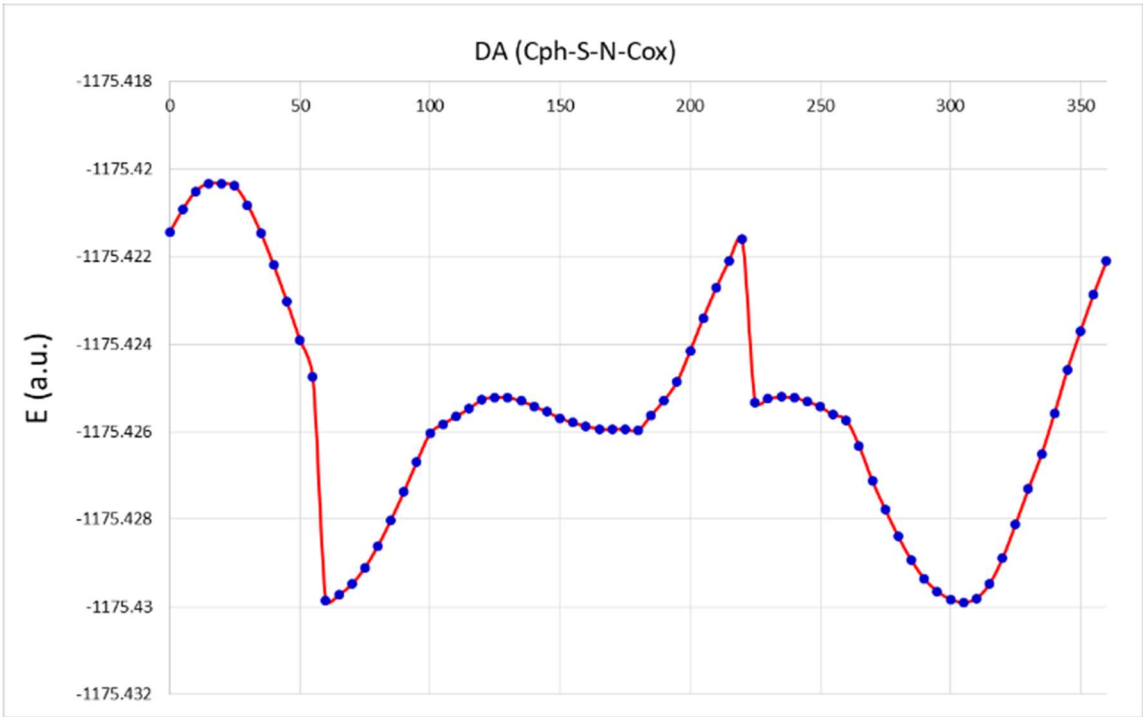

Fig. 1. The ωB97XD/6-31G(d) computed molecular energies for scanning of C_{Ph}-S-N-C_{ox} dihedral angle of **SMX**.

An overview of the diagram presented in Fig. 1, shows that by rotation of **SMX** around the C_{Ph}-S-N-C_{ox} dihedral angle, two minima are observed at 60 and 305°. Thus, the conformer relevant to the dihedral angle of 305° (which is very slightly more stable relative to that of 60°) was considered for further studies. In this conformer, the aromatic rings are located mutually near. The structure of this conformer is depicted in Fig. 2.

Adsorption and Solvation Energies and Thermodynamics Parameters

In the current work, the adsorption of **SMX** drug on the pristine C_{60} and its functionalized form *i.e.* $C_{60}HNH_2$ has been studied to clarify whether these adsorbents can be potentially applicable for drug delivery of **SMX**. Figure 2 depicts the optimized forms of **SMX**, C_{60}, and $C_{60}HNH_2$.

In the first step, different adsorption situations of **SMX** on the C_{60} fullerene were designed as follows:

a) **SMX**-pristine-C_{60}:

1. NH_2 group near the fullerene; 2. Six-membered ring, NH_2, and SO_2 groups near the fullerene; 3. NH and SO_2 groups near the fullerene; 4. Five-membered ring and NH group near the fullerene.

b) **SMX**- $C_{60}HNH_2$:

1. Drug NH_2 group near the NH_2 group of the fullerene; 2. SO_2 oxygen atom near the hydrogen atom in the NH_2 group of the fullerene; 3. SO_2 oxygen atom and nitrogen atom near the hydrogen atom in the NH_2 group of the fullerene; 4. Nitrogen atom near the hydrogen atom in the NH_2 group of the fullerene; 5. Nitrogen and oxygen atoms in the five-membered ring near the NH_2 group of the fullerene; 6. Nitrogen atom in the five-membered ring near the NH_2 group of the fullerene; 7. Hydrogen atom in the NH group near the NH_2 group of the fullerene; 8. Six-membered ring near the fullerene; 9. Five-membered ring near the fullerene; 10. SO_2 oxygen atom near the hydrogen atom of the fullerene, hydrogen atom in the NH group near the nitrogen atom in the NH_2 group of the fullerene; 11. SO_2 oxygen atom near the hydrogen atom in the NH_2 group of the fullerene, the nitrogen atom in the NH group near the hydrogen atom of the fullerene; 12. Nitrogen atom in the NH group near the hydrogen atom in the NH_2 group of the fullerene, nitrogen atom in the five-membered ring near the hydrogen atom of the fullerene; 13. Six-membered ring near the NH_2 group of the fullerene.

Fig. 2. The optimized structures of **SMX**, C_{60} and $C_{60}HNH_2$.

Table 1. Different Adsorption Situations of **SMX** on the C_{60} Fullerene Together with the Corresponding Parameters Including Gibbs Free Energies ΔG_{ads}, Enthalpies ΔH_{ads}, Entropies ΔS_{ads} and Adsorption Energies ΔE_{ads} in the Gas Phase (Values in Parenthesis) and Aqueous Solution at Room Temperature. The Adsorption Situations are Given in S1

Entry	ΔG (kJ mol^{-1})	ΔH (kJ mol^{-1})	ΔS (kJ K^{-1} mol^{-1})	ΔE_{ads} (kJ mol^{-1})
1	6.01	-34.36	-0.135	-40.12
	(11.86)	(-35.92)	(-0.160)	(-43.81)
2	16.18	-38.02	-0.182	-40.96
	(9.38)	(-39.25)	(-0.163)	(-44.81)
3	20.46	-33.06	-0.179	-36.36
	(15.54)	(-36.93)	(-0.176)	(-39.35)
4[a]	-	-	-	-
	(8.30)	(-36.64)	(-0.151)	(-41.91)

Then, corresponding thermodynamic parameters including Gibbs free energies, enthalpies, and entropies were calculated after optimization of the geometries. Also, the adsorption energies ΔE_{ads} were calculated by using Eq. (1).

The calculations were carried out in both gaseous and aqueous phases at room temperature. Table 1 summarizes the different adsorption situations of **SMX** on the C_{60} fullerene together with the corresponding parameters including Gibbs free energies ΔG_{ads}, enthalpies ΔH_{ads}, entropies ΔS_{ads} and adsorption energies ΔE_{ads} in both gas phase and solution.

An analysis of the results presented in Table 1 suggests that:

1) For both gas and solution phases and in all situations, the enthalpies and adsorption energies are negative in value indicating the adsorption process is exothermic.

2) The entropies are decreased during the adsorption process due to the reduction of the freedom degrees of the interacting species.

3) The Gibbs free energies are positive in values suggesting that the adsorption process is unfavorable for all situations, which can be attributed to the overcoming of the unfavorable entropy term on the enthalpy one.

Thus, apparently, the pristine C_{60} fullerene cannot be considered as a suitable adsorbent for **SMX** drug.

At the next step, the adsorption of **SMX** drug on a functionalized C_{60}, namely $C_{60}HNH_2$, was studied to evaluate the effect of the functional groups on the adsorption process. The results for the adsorption of **SMX** drug on $C_{60}HNH_2$ are given in Table 2 for solution and gaseous phases at room temperature.

Table 2. Different Adsorption Situations of **SMX** on $C_{60}HNH_2$ Together with the Corresponding Parameters Including Gibbs Free Energies ΔG_{ads}, Enthalpies ΔH_{ads}, Entropies ΔS_{ads} and Adsorption Energies ΔE_{ads} in the Gas Phase (Values in Parenthesis) and Aqueous Solution at Room Temperature. The Adsorption Situations are Presented in S2

Entry	ΔG (kJ mol^{-1})	ΔH (kJ mol^{-1})	ΔS (kJ K^{-1} mol^{-1})	ΔE_{ads} (kJ mol^{-1})	ΔE_{solv} (kJ mol^{-1})
1	2.18	-49.40	-0.173	-56.78	-61.03
	(-3.36)	(-58.49)	(-0.185)	(-66.26)	
2	6.94	-41.47	-0.162	-47.72	-61.96
	(-3.63)	(-50.23)	(-0.156)	(-56.28)	
3	8.96	-39.40	-0.162	-45.92	-91.50
	(17.90)	(-18.85)	(-0.123)	(-24.94)	
4	1.12	-47.10	-0.162	-52.83	-55.70
	(-18.02)	(-62.61)	(-0.150)	(-67.64)	
5	9.01	-37.11	-0.155	-42.92	-60.68
	(1.05)	(-46.85)	(-0.161)	(-52.76)	
6	4.90	-42.17	-0.158	-48.43	-60.58
	(-1.61)	(-51.70)	(-0.168)	(-58.36)	
7	-10.34	-60.17	-0.167	-65.78	-57.73
	(-16.44)	(-75.37)	(-0.198)	(-78.57)	
8	4.77	-43.72	-0.163	-49.62	-61.94
	(-3.25)	(-52.26)	(-0.164)	(-58.20)	
9	6.56	-45.47	-0.174	-48.39	-61.60
	(-0.63)	(-51.00)	(-0.169)	(-57.31)	
10	-14.63	-60.25	-0.153	-65.70	-59.13
	(-25.50)	(-71.42)	(-0.154)	(-77.08)	
11	11.38	-44.47	-0.187	-47.46	-58.64
	(-6.20)	(-54.00)	(-0.160)	(-59.33)	
12	5.68	-38.24	-0.147	-44.50	-59.83
	(-1.02)	(-49.04)	(-0.161)	(-55.19)	
13	0.88	-51.96	-0.177	-59.48	-50.00
	(-15.79)	(-71.74)	(0.188)	(-80.00)	

An analysis of the results summarized in Table 2 suggests that the adsorption energies and enthalpies are negative for all situations showing that the adsorption process is exothermic. On the other hand, the Gibbs free energies are negative only for situations 7 and 10, which indicates that the adsorption process is favorable for these situations. Although, both situations possess identical values for adsorption energies (~ -66.00 kJ mol^{-1}), situation 10 with a more negative value of Gibbs free energy (-14.63 against -10.34 kJ mol^{-1}) is more favorable relative to 7 one. In addition, a comparison between the results of Gibbs free energies for the gas phase relative to the solution indicates that in contrast to the solution, the adsorption processes are more favorable in the gas phase. This probably can be attributed to the formation of the hydrogen bond between the water as solvent and **SMX** or $C_{60}HNH_2$ in solution which reduces the strength of intermolecular interactions between **SMX** and $C_{60}HNH_2$. However, such solvent hydrogen bonds are absent in the gas phase and the **SMX** … $C_{60}HNH_2$ interaction becomes important [45].

A comparison between the results obtained for the adsorption of **SMX** on pristine C_{60} (Table 1) with those obtained for functionalized fullerene $C_{60}HNH_2$ (Table 2) clearly indicates that the functionalization of the fullerene with the polar groups improves significantly the adsorption process because of appearance of the stronger attraction forces between the interacting species.

Meanwhile, the solvation energy values were calculated by Eq. (2) and given in Table 2. The high solvation energy of the adsorbed drug on fullerenes strengthens their applicability as nano-carriers in drug delivery systems [41]. As stated above, among the interactions between **SMX** and $C_{60}HNH_2$, only situations 7 and 10 are spontaneous and favorable, and among them, in agreement with the Gibbs energy, situation 10 has more negative solvation energy than situation 7, therefore, it seems to be more suitable for the drug delivery systems.

IGMH Analysis on the Adsorption Process

Recently, Hénon *et al.* introduced an independent gradient model (IGM) to analyze interaction regions between two interacting species. To identify visually different types of interactions, the interaction regions are presented by using different values of the isosurface δg function and sign(λ_2)ρ as a mapped function [42]. Then, the new version of IGM, namely IGMH, was proposed by Lu and coworkers in 2022 in terms of the Hirshfeld partition of actual molecular density [46]. In the last method, free-state atomic densities in the IGM method are replaced by atomic densities obtained from the Hirshfeld partition of actual molecular electron density. Thus, at the next step, the adsorption process was analyzed by the IGMH method in order to evaluate the interactions.

Since for adsorption of **SMX** on the pristine C_{60} and $C_{60}HNH_2$, situations 1 (in Table 1) and 10 (in Table 2) gave the best results, the IGMH analysis was performed on these geometries in solution. Figure 3, depicts the color-mapped isosurfaces of the inter-fragment IGMH for the above-mentioned situations together with the colored scale bar.

The appearance of an extended green isosurface between the phenyl ring of **SMX** and the pristine C_{60} fullerene portrayed in sections A and B of Fig. 3, clearly suggests the presence of an interaction between the two fragments. According to the colored scale, this interaction is classified as a weak van der Waals attraction, which explains the weak adsorption

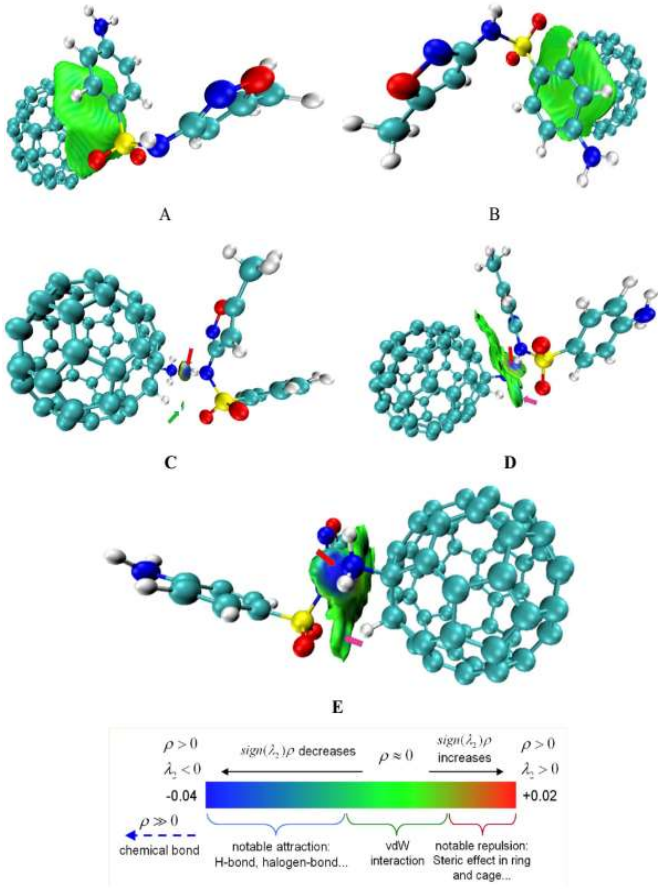

Fig. 3. Representation of IGMH isosurfaces portraying interactions between **SMX** and pristine C_{60} (A and B) as well as $C_{60}HNH_2$ (C, D, and E) in solution together with the colored scale bar.

between the two molecules. Due to the presence of the π-system in the phenyl ring of **SMX** as well as in the C_{60} fullerene, the corresponding interaction can be considered as a π…π stacking one.

IGMH analysis on the adsorption of **SMX** on functionalized $C_{60}HNH_2$ for the situation 10 (sections C, D, and E in Fig. 3) suggests stronger interactions relative to the adsorption of **SMX** on the pristine C_{60} fullerene. The most important interaction is observed between the hydrogen atom of NH in **SMX** and the nitrogen atom of the NH_2 group in $C_{60}HNH_2$ with the appearance of a blue isosurface in this region, which is portrayed with a red arrow. According to the colored scale, the appearance of such isosurface is indicative the presence of a hydrogen bond. In addition, the presence of

a green isosurface between the oxygen atom of the SO_2 group in **SMX** and the hydrogen atom of the C-H group in $C_{60}HNH_2$ specified by a pink arrow suggests a weak van der Waals interaction for this region.

Figure 4 depicts the two-dimensional diagram of $\delta^{ginter/intra}$ against sign($\lambda 2$)ρ for adsorption situation 10 of **SMX** on $C_{60}HNH_2$.

Taking Fig. 4 into account, the presence of a red spike around sign(λ_2)ρ = -0.040 a.u. suggests the formation of a hydrogen bond between the hydrogen atom of NH in **SMX** and the nitrogen atom of the NH_2 group in $C_{60}HNH_2$. In addition, the presence of a short spike in the right hand of the N…H spike, is attributed to the O…H interaction between the oxygen atom of the SO_2 group in **SMX** and the hydrogen atom of the C-H group in $C_{60}HNH_2$. This interaction is weaker relative to the N…H one because it possesses a more positive value of sign(λ_2)ρ.

Charge Transfer Study in Adsorption

Since the interaction of the molecules is usually accompanied by charge transfer, the magnitude of this parameter can affect the interaction energies. Global electron density transfer (GEDT) can be considered as a criterion for the evaluation of charge transfer and polarity of the species. Thus, at the next step, the GEDT values were calculated for the most favorable adsorption of **SMX** on both pristine C_{60} and $C_{60}HNH_2$, which the results are given in Fig. 5 along with the corresponding molecular electrostatic potential (MEP) map. In a MEP map, the regions with high and low electron density are represented by red and blue colors, respectively.

Given the results in Fig. 5, the GEDT value for adsorption of **SMX** on pristine C_{60} was found to be 0.014 *e*, in which the electron density fluxes from **SMX** toward the fullerene. It is expected that this adsorption is weak because of the low value of GEDT. The adsorption energies given in Table 1 also confirm this conclusion. The appearance of a dark blue region on the phenyl group of **SMX**, the adsorption region, confirms electron transfer from **SMX** toward fullerene. On the other hand, for the adsorption of **SMX** on the functionalized fullerene, there are two important issues. First, the GEDT value is increased approximately four times relative to the adsorption on C_{60}, which is responsible for stronger adsorption in agreement with adsorption energies summarized in Table 1, and second, in contrast to the adsorption on C_{60}, the electron density fluxes from the $C_{60}HNH_2$ toward **SMX**. The appearance of a dark blue region around the NH_2 group in $C_{60}HNH_2$ and a red one around the sulfonamide group in **SMX** confirms electron transfer from the former toward the latter.

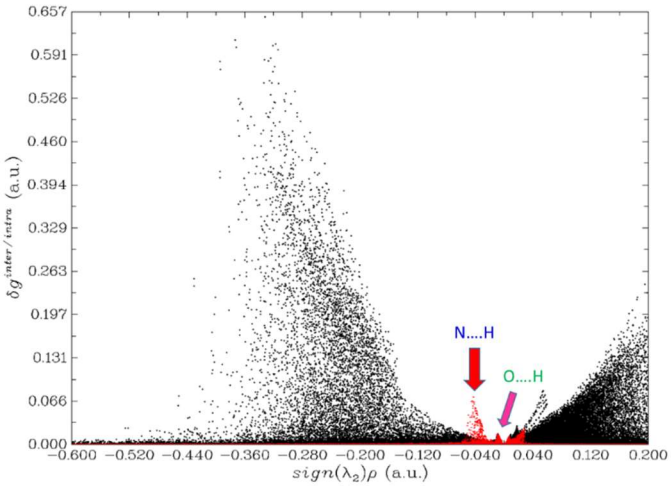

Fig. 4. Two-dimensional diagram of $\delta^{ginter/intra}$ against sign($\lambda 2$)ρ for adsorption of **SMX** on $C_{60}HNH_2$. The black and red points refer to δg^{intra} and δg^{inter}, respectively.

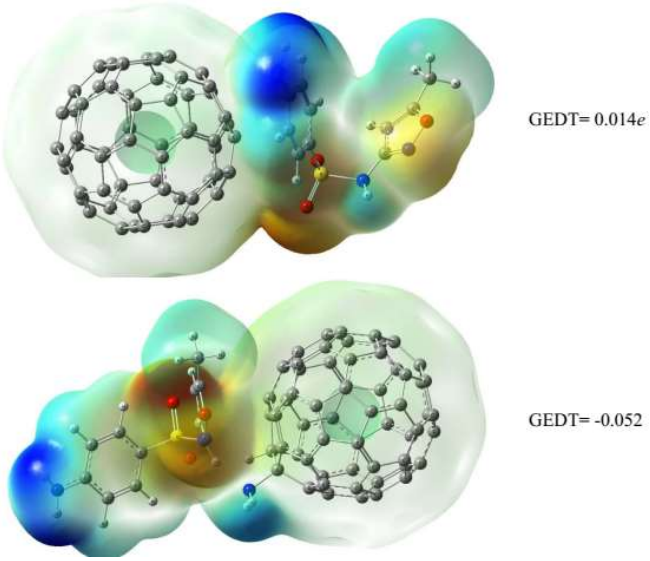

Fig. 5. Molecular electrostatic potential (MEP) map along with the GEDT values for the most favorable adsorption of SMX on both pristine C_{60} (up, situation 1) and $C_{60}HNH_2$ (down, situation 10).

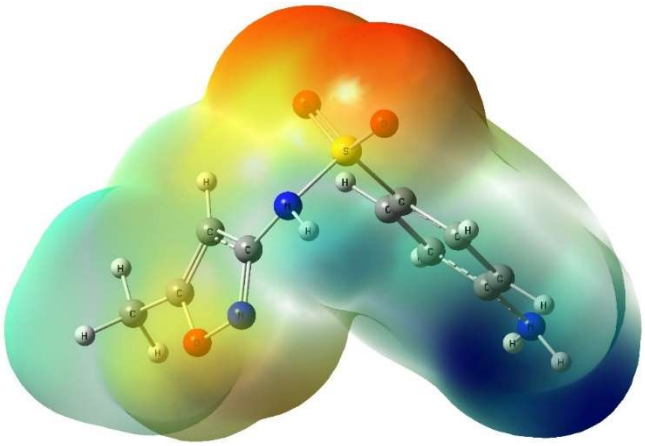

Fig. 6. Molecular electrostatic potential map for **SMX** obtained by ωB97XD/6-31G(d) method.

Figure 6 shows the MEP map for **SMX**. It is clear that the region around the SO_2 group is red which suggests high electron density. Thus, the oxygen atoms of this group can interact with the hydrogen atom of the C_{60}**H**NH_2 which is confirmed by the IGMH analysis in the adsorption situation 10. Also, this region along with the six-membered ring can interact with the pristine C_{60} fullerene.

To Study the Possibility of Chemical Adsorption *via* [4+2] Cycloaddition of Fullerene and SMX

Since the five-membered ring in **SMX** possesses two conjugated double bonds, it may participate in [4+2] cycloaddition reaction as a diene. On the other hand, the C60 fullerene can participate in such reactions as a dienophile [47, 48].

Thus, at the next step, the [4+2] cycloaddition reaction of the pristine and functionalized C_{60} fullerenes with **SMX** was studied in order to shed light on the possibility of chemical adsorption (Scheme 2). For the pristine fullerene C_{60}, one cycloaddition reaction and for the functionalized fullerene, $C_{60}HNH_2$, 16 cycloaddition reaction paths were considered and the geometries of the [4+2] cycloadducts and the corresponding transition states were optimized. Table 3 summarizes the optimized geometries of the transition states and products and the corresponding kinetics and thermodynamics parameters including relative Gibbs free energies, enthalpies, and entropies in the presence of water at room temperature.

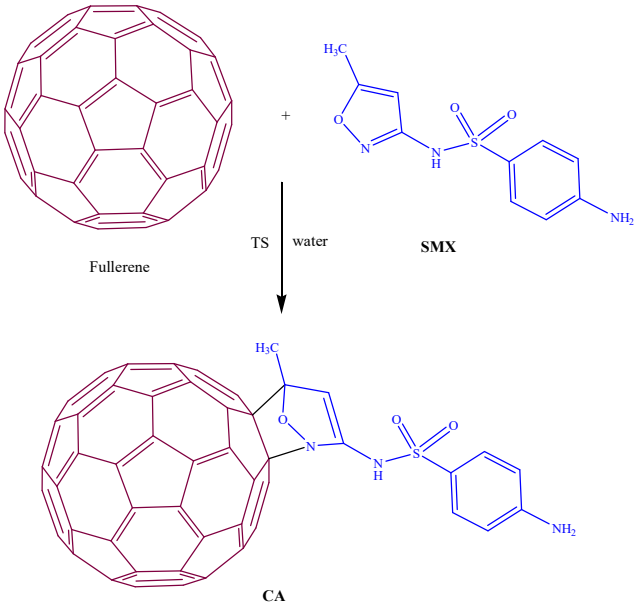

Scheme 2. [4+2] cycloaddition reaction of the fullerene as dienophile with **SMX** as diene

An overview of the results summarized in Table 3 suggests that all reaction paths are endothermic with high activation barriers. However, among the reaction paths, that which is related to the interaction of the C3-C4 bond of $C_{60}HNH_2$ (relative to the C1 carbon atom possessing NH_2 group) with **SMX** has less activation barrier and is less endothermic relative to the others. In addition, due to the reduction of the freedom degrees of the reactants, all entropies are negative values. Accordingly, due to the unfavorable enthalpies and entropies, the cycloaddition reaction of **SMX** with the pristine and functionalized fullerenes is ruled out.

CONCLUSIONS

In this study, the interaction of sulfamethoxazole drug on the pristine and functionalized C_{60} fullerenes in different situations was calculated by density functional theory. The calculations showed unfavorable adsorption of sulfamethoxazole on the pristine C_{60} surface but based on the adsorption and Gibbs energies, its adsorption on the functionalized fullerene ($C_{60}HNH_2$) was spontaneous and favorable, in two situations. Among these situations, the

Table 3. Optimized Geometries of Transition States (TSs) and Cycloadducts (CAs) of the [4+2] Cycloaddition Reaction between the **SMX** and C60 as well as $C_{60}HNH_2$ Together with the Kinetics and Thermodynamics Parameters in the Presence of Water at Room Temperature. The Adsorption Situations are Given in S3

Reaction path[a]	$\Delta H^{\ddagger}$ (kJ mol^{-1})	$\Delta S^{\ddagger}$ (kJ mol^{-1})	$\Delta G^{\ddagger}$ (kJ mol^{-1})	ΔH_r (kJ mol^{-1})	ΔS_r (kJ mol^{-1})	ΔG_r (kJ mol^{-1})
1	167.98	-0.212	230.99	126.14	-0.221	191.75
1	271.24	-0.219	336.15	260.98	-0.206	322.13
2	94.58	-0.209	156.75	13.17	-0.232	82.15
3	139.52	-0.228	207.34	69.92	-0.224	136.44
4	114.03	-0212	177.09	28.17	-0.231	96.72
5	264.70	-0.215	328.67	254.05	-0.223	230.30
6	108.79	-0.209	171.12	28.77	-0.210	93.28
7	155.76	-0.211	218.52	102.22	-0.228	170.07
8	290.56	-0.207	252.27	157.98	-0.225	224.85
9	167.06	-0.217	231.51	116.10	-0.230	184.54
10	178.33	-0.217	242.86	128.27	-0.227	195.78
11	208.87	-0.209	271.03	179.39	-0.223	245.76
12	175.84	-0.227	243.36	126.09	-0.230	194.49
13	180.34	-0.219	245.45	138.88	-0.228	206.60
14	175.40	-0.215	239.50	134.78	-0.224	201.38
15	173.46	-0.213	236.94	130.11	-0.215	194.22
16	107.56	-0.214	170.98	38.61	-0.227	106.03

[a]The first row is related to the reaction of **SMX** with C_{60} and the further rows are related to that with $C_{60}HNH_2$.

situation 10 (SO_2 oxygen atom near to hydrogen atom of the fullerene, hydrogen atom in NH group near the nitrogen atom in NH_2 group of the fullerene) is more favorable relative to 7 one (hydrogen atom in NH group near to NH_2 group of the fullerene) due to be more negative value of Gibbs free energy (-14.63 against -10.34 kJ mol^{-1}). In addition, a comparison between Gibbs free energies in the gas and solution phases indicated that in contrast to the solution, the adsorption process is more favorable in the gas phase. This probably can be attributed to the formation of the hydrogen bond between the water as solvent and **SMX** or $C_{60}HNH_2$ in solution which reduces the strength of intermolecular interactions between **SMX** and $C_{60}HNH_2$. Also, in agreement with the Gibbs energy, the functionalized C_{60} in two situations, has negative solvation energy, therefore, it can be suitable as the nano-carrier in drug delivery systems. In addition, analysis of the interaction of sulfamethoxazole with the functionalized C_{60}, in the most favorable situation, by the independent gradient model based on Hirshfeld partition (IGMH) confirmed the strong interaction between the two fragments of **SMX** and $C_{60}HNH_2$. Meanwhile, the analysis of the global electron density transfer (GEDT) showed that the electron density fluxes from **SMX** toward the fullerene for the C_{60}, and vice versa for the $C_{60}HNH_2$. The possibility of chemical adsorption of **SMX** on the pristine and functionalized fullerenes using [4+2] cycloaddition reactions was also investigated and the resulting thermodynamic and kinetics parameters ruled out such adsorption.

REFERENCES

[1] Shi, J.; Votruba, A. R.; Farokhzad, O. C.; Langer, R., Nanotechnology in drug delivery and tissue engineering: from discovery to applications. *Nano Lett.* **2010**, *10*, 3223-3230. DOI: 10.1021/nl102184c.

[2] Farokhzad, O. C.; Langer, R., Impact of nanotechnology

on drug delivery. *ACS Nano* **2009**, *3*, 16-20. DOI: 10.1021/nn900002m.

[3] Koo, O. M.; Rubinstein, I.; Onyuksel, H., Role of nanotechnology in targeted drug delivery and imaging: a concise review. *Nanomedicine: Nanotechnol. Biol. Med.* **2005**, *1*, 193-212. DOI: 10.1016/j.nano.2005.06.004.

[4] Colson, P.; Rolain, J. -M.; Raoult, D., Chloroquine for the 2019 novel coronavirus SARS-CoV-2, Elsevier, **2020**, p. 105923.

[5] Parlak, C.; Alver, Ö., A density functional theory investigation on amantadine drug interaction with pristine and B, Al, Si, Ga, Ge doped C60 fullerenes. *Chem. Phys. Lett.* **2017**, *678*, 85-90. DOI: 10.1016/j.cplett.2017.04.025.

[6] Shah, A.; Kashyap, R.; Tosh, P.; Sampathkumar, P.; O'Horo, J. C., Guide to understanding the 2019 novel coronavirus, Mayo Clinic Proceedings, Elsevier, **2020**, pp. 646-652.

[7] De Jong, W. H.; Borm, P. J., Drug delivery and nanoparticles: applications and hazards. *Int. J. Nanomedicine* **2008**, *3*, 133-149. DOI: 10.2147/ijn.s596.

[8] Conti, M.; Tazzari, V.; Baccini, C.; Pertici, G.; Serino, L. P.; De Giorgi, U., Anticancer drug delivery with nanoparticles. *In Vivo* **2006**, *20*, 697-701.

[9] Singh, R.; Lillard Jr, J. W., Nanoparticle-based targeted drug delivery. *Exp. Mol. Pathol.* **2009**, *86*, 215-223. DOI: 10.1016/j.yexmp.2008.12.004.

[10] Bakry, R.; Vallant, R. M.; Najam-ul-Haq, M.; Rainer, M.; Szabo, Z.; Huck, C. W.; Bonn, G. K., Medicinal applications of fullerenes. *Int. J. Nanomedicine* **2007**, *2*, 639-649. DOI: 10.2147/IJN.S2.4.639.

[11] Shi, J.; Zhang, H.; Wang, L.; Li, L.; Wang, H.; Wang, Z.; Li, Z.; Chen, C.; Hou, L.; Zhang, C., PEI-derivatized fullerene drug delivery using folate as a homing device targeting to tumor. *Biomater.* **2013**, *34*, 251-261. DOI: 10.1016/j.biomaterials.2012.09.039.

[12] Fan, J.; Fang, G.; Zeng, F.; Wang, X.; Wu, S., Water-dispersible fullerene aggregates as a targeted anticancer prodrug with both chemo-and photodynamic therapeutic actions. *Small* **2013**, *9*, 613-621. DOI: 10.1002/smll.201201456.

[13] Chow, E. K. -H.; Ho, D., Cancer nanomedicine: from drug delivery to imaging. *Sci. Transl. Med.* **2013**, *5*, 216rv4-216rv4, DOI: 10.1126/scitranslmed.3005872.

[14] Zou, Y.; Zhang, X.; Li, Y.; Wang, B.; Yan, H.; Cui, J.; Liu, L.; Da, D., Bonding character of the boron-doped C 60 films prepared by radio frequency plasma assisted vapor deposition. *J. Mater. Sci.* **2002**, *37*, 1043-1047, DOI: 10.1023/A:1014368418784.

[15] de Leon, A.; Jalbout, A. F.; Basiuk, V. A., Fullerene-amino acid interactions. A theoretical study. *Chem. Phys. Lett.* **2008**, *452*, 306-314. DOI: 10.1016/j.cplett.2007.12.065.

[16] Shariatinia, Z.; Shahidi, S., A DFT study on the physical adsorption of cyclophosphamide derivatives on the surface of fullerene C60 nanocage. *J. Mol. Graphics Modell.* **2014**, *52*, 71-81. DOI: 10.1016/j.jmgm.2014.06.001.

[17] Hazrati, M. K.; Hadipour, N. L., Adsorption behavior of 5-fluorouracil on pristine, B-, Si-, and Al-doped C60 fullerenes: A first-principles study. *Phys. Lett. A* **2016**, *380*, 937-941. DOI: 10.1016/j.physleta.2016.01.020.

[18] Bashiri, S.; Vessally, E.; Bekhradnia, A.; Hosseinian, A.; Edjlali, L., Utility of extrinsic [60] fullerenes as work function type sensors for amphetamine drug detection: DFT studies. *Vacuum* **2017**, *136*, 156-162. DOI: 10.1016/j.vacuum.2016.12.003.

[19] Rad, A. S.; Aghaei, S. M.; Aali, E.; Peyravi, M., Study on the electronic structure of Cr-and Ni-doped fullerenes upon adsorption of adenine: a comprehensive DFT calculation. *Diamond Relat. Mater.* **2017**, *77*, 116-121. DOI: 10.1016/j.diamond.2017.06.013.

[20] Parlak, C.; Alver, Ö.; Şenyel, M., Computational study on favipiravir adsorption onto undoped-and silicon-decorated C60 fullerenes. *J. Theor. Comput. Chem.* **2017**, *16*, 1750011. DOI: 10.1142/S0219633617500110.

[21] Moradi, M.; Nouraliei, M.; Moradi, R., Theoretical study on the phenylpropanolamine drug interaction with the pristine, Si and Al doped [60] fullerenes. *Physica E: Low-dimensional Systems and Nanostructures* **2017**, *87*, 186-191. DOI: 10.1016/j.physe.2016.11.027.

[22] Samanta, P. N.; Das, K. K., Noncovalent interaction assisted fullerene for the transportation of some brain anticancer drugs: a theoretical study. *J. Mol. Graphics Modell.* **2017**, *72*, 187-200. DOI: 10.1016/j.jmgm.2017.01.009.

[23] Ergürhan, O.; Parlak, C.; Alver, Ö.; Şenyel, M., Conformational and electronic properties of

hydroquinone adsorption on C60 fullerenes: Doping atom, solvent and basis set effects. *J. Mol. Struct.* **2018**, *1167*, 227-231. DOI: 10.1016/j.molstruc.2018.04.092.

[24] Ghasemi, A. S.; Mashhadban, F.; Ravari, F., A DFT study of penicillamine adsorption over pure and Al-doped C 60 fullerene. *Adsorption* **2018**, *24*, 471-480. DOI: 10.1007/s10450-018-9960-3.

[25] Fekri, M. H.; Bazvand, R.; Soleymani, M.; Razavi Mehr, M., Adsorption of Metronidazole drug on the surface of nano fullerene C60 doped with Si, B and Al: A DFT study. *Int. J. Nano Dimens.* **2020**, *11*, 346-354.

[26] Fekri, M. H.; Bazvand, R.; Solymani, M.; Razavi Mehr, M., Adsorption behavior, electronical and thermodynamic properties of ornidazole drug on C60 fullerene doped with Si, B and Al: A quantum mechanical simulation. *Phys. Chem. Res.* **2021**, *9*, 151-164. DOI: 10.22036/PCR.2020.244279.1814.

[27] Bilge, M., A DFT investigation of the interaction of B-and Al-doped C 60 fullerenes with cyclopropylpipezarine. *J. Struct. Chem.* **2018**, *59*, 1271-1275. DOI: 10.1134/S0022476618060045.

[28] Behmanesh, A.; Salimi, F.; Ebrahimzadeh Rajaei, G., Adsorption behavior of letrozole on pure, Ge-and Si-doped C 60 fullerenes: a comparative DFT study. *Monatsh. Chem. Chem. Mon.* **2020**, *151*, 25-32. DOI: 10.1007/s00706-019-02524-1.

[29] Ghasemi, A.; Ashrafi, F.; Babanejad, S.; Elyasi, A., Study of the Physicochemical Properties of Anti-Cancer Drug Gemcitabine on the Surface of Al Doped C 60 and C 70 Fullerenes: A DFT Computation. *J. Struct. Chem.* **2019**, *60*, 13-19. DOI: 10.1134/S0022476619010037.

[30] Novir, S. B.; Aram, M. R., Quantum mechanical simulation of Chloroquine drug interaction with C60 fullerene for treatment of COVID-19. *Chem. Phys. Lett.* **2020**, *757*, 137869. DOI: 10.1016/j.cplett.2020.137869.

[31] Kamali, F.; Ebrahimzadeh Rajaei, G.; Mohajeri, S.; Shamel, A.; Khodadadi-Moghaddam, M., Adsorption behavior of metformin drug on the C 60 and C 48 nanoclusters: a comparative DFT study. *Monatsh. Chem. Chem. Mon.* **2020**, *151*, 711-720. DOI: 10.1007/s00706-020-02597-3.

[32] Bhattacharjee, M. K., Antimetabolites: Antibiotics That Inhibit Nucleotide Synthesis, Chemistry of Antibiotics and Related Drugs, Springer, **2022**, pp. 109-123.

[33] Zhang, Y.; Meshnick, S., Inhibition of Plasmodium falciparum dihydropteroate synthetase and growth in vitro by sulfa drugs. *Antimicrob. Agents Chemother.* **1991**, *35*, 267-271. DOI: 10.1128/aac.35.2.267.

[34] Frisch, M. J., Trucks, G. W., Schlegel, H. B., Scuseria, G. E., Robb, M. A., Cheeseman, J. R., Scalmani, G., Barone, V., Mennucci, B., Petersson, G. A., Nakatsuji, H., Caricato, M., Li, X., Hratchian, H. P., Izmaylov, A. F., Bloino, J., Zheng, G., Sonnenberg, J. L., Hada, M., Ehara, M., Toyota, K., Fukuda, R., Hasegawa, J., Ishida, M., Nakajima, T., Honda, Y., Kitao, O., Nakai, H., Vreven, T., Montgomery, J. A., Jr., Peralta, J. E., Ogliaro, F., Bearpark, M., Heyd, J. J., Brothers, E., Kudin, K. N., Staroverov, V. N., Kobayashi, R., Normand, J., Raghavachari, K., Rendell, A., Burant, J. C., Iyengar, S. S., Tomasi, J., Cossi, M., Rega, N., Millam, J. M., Klene, M., Knox, J. E., Cross, J. B., Bakken, V., Adamo, C., Jaramillo, J., Gomperts, R., Stratmann, R. E., Yazyev, O., Austin, A. J., Cammi, R., Pomelli, C., Ochterski, J. W., Martin, R. L., Morokuma, K., Zakrzewski, V. G., Voth, G. A., Salvador, P., Dannenberg, J. J., Dapprich, S., Daniels, A. D., Farkas, Ö., Foresman, J. B., Orti, Gussian 09, Revision E. 01 [CD]. Wallingford CT: Gaussian, Inc, **2009**.

[35] Cammi, R.; Mennucci, B.; Tomasi, J., Solvent effects on linear and nonlinear optical properties of donor−acceptor polyenes: investigation of electronic and vibrational components in terms of structure and charge distribution changes. *J. Am. Chem. Soc.* **1998**, *120*, 8834-8847. DOI: 10.1021/ja980823c.

[36] Cammi, R.; Mennucci, B.; Tomasi, J., On the calculation of local field factors for microscopic static hyperpolarizabilities of molecules in solution with the aid of quantum-mechanical methods. *J. Phys. Chem. A* **1998**, *102*, 870-875, DOI: 10.1021/jp9726807.

[37] Mennucci, B.; Martínez, J. M.; Tomasi, J., Solvent effects on nuclear shieldings: Continuum or discrete solvation models to treat hydrogen bond and polarity effects? *J. Phys. Chem. A* **2001**, *105*, 7287-7296, DOI: 10.1021/jp010837w.

[38] Cammi, R.; Mennucci, B.; Tomasi, J., An attempt to bridge the gap between computation and experiment for nonlinear optical properties: macroscopic susceptibilities in solution. *J. Phys. Chem. A* **2000**, *104*, 4690-4698,

DOI: 10.1021/jp994163p.

[39] Mennucci, B.; Tomasi, J.; Cammi, R.; Cheeseman, J.; Frisch, M.; Devlin, F.; Gabriel, S.; Stephens, P., Polarizable continuum model (PCM) calculations of solvent effects on optical rotations of chiral molecules. *J. Phys. Chem. A* **2002**, *106*, 6102-6113. DOI: 10.1021/jp020124t.

[40] Amovilli, C.; Barone, V.; Cammi, R.; Cances, E.; Cossi, M.; Mennucci, B.; Pomelli, C.; Tomasi, J.; Lowdin, P.; Sabin, J., Advances in quantum chemistry. *Adv. Quantum Chem.* **1998**, *32*, 227-61. DOI: 10.1016/S0065-3276(08)60416-5.

[41] Singla, P.; Riyaz, M.; Singhal, S.; Goel, N., Theoretical study of adsorption of amino acids on graphene and BN sheet in gas and aqueous phase with empirical DFT dispersion correction. *Phys. Chem. Chem. Phys.* **2016**, *18*, 5597-5604, DOI: 10.1039/C5CP07078C.

[42] Lu, T.; Chen, Q., Independent gradient model based on Hirshfeld partition: A new method for visual study of interactions in chemical systems. *J. Comput. Chem*. **2022**, *43*, 539-555. DOI: 10.1002/jcc.26812.

[43] Reed, A. E.; Weinstock, R. B.; Weinhold, F., Natural population analysis. *J. Chem. Phys* **1985**, *83*, 735-746, DOI: 10.1063/1.449486.

[44] Reed, A. E.; Curtiss, L. A.; Weinhold, F., Intermolecular interactions from a natural bond orbital, donor-acceptor viewpoint. *Chem. Rev.* **1988**, *88*, 899-926, DOI: 10.1021/cr00088a005.

[45] Dashti Khavidaki, H.; Soleymani, M., A DFT Study on Adsorption of Alanine on Pristine, Functionalized and Boron and/or Nitrogen Doped Functionalized C60 Fullerenes. *Phys. Chem. Res.* **2020**, *8*, 657-669. DOI: 10.22036/PCR.2020.227279.1759.

[46] Lu, T.; Chen, Q., Independent gradient model based on Hirshfeld partition: A new method for visual study of interactions in chemical systems. *J. Comput. Chem.* **2022**, *43*, 539-555. DOI: 10.1002/jcc.26812.

[47] Sarova, G. H.; Berberan-Santos, M. N., Kinetics of the Diels-Alder reaction between C60 and acenes. *Chem. Phys. Lett.* **2004**, *397*, 402-407. DOI: 10.1016/j.cplett.2004.09.005.

[48] Wang, G. -W.; Chen, Z. -X.; Murata, Y.; Komatsu, K., [60] Fullerene adducts with 9-substituted anthracenes: mechanochemical preparation and retro Diels-Alder reaction. *Tetrahedron* **2005**, *61*, 4851-4856. DOI: 10.1016/j.tet.2005.02.089.